XV International Conference on Computational Plasticity. Fundamentals and Applications
COMPLAS 2019
E. Oñate, D.R.J. Owen, D. Peric, M. Chiumenti & Eduardo de Souza Neto (Eds)

A NOVEL INDICATOR FOR KINEMATIC HARDENING EFFECT QUANTIFICATION IN DEEP DRAWING SIMULATION

RÉMI LAFARGE*, NIKLAS KÜSTERS* AND ALEXANDER BROSIUS*

* Chair of Forming and Machining Processes (FF)
Technische Universität Dresden (TUD)
01069 Dresden, Germany
e-mail: remi.lafarge@mailbox.tu-dresden.de, web page: http://www.tu-dresden.de/mw/if/ff

Key words: Sheet metal forming, kinematic hardening

Abstract. Deep drawing simulation techniques reduce tool design costs and improve tool performance and reliability. In terms of strain hardening, mixed models capturing the kinematic effect are sometimes more accurate than isotropic models. Indeed, non-linearity in strain paths can lead to inconsistent simulation results. However, the use of such models requires a greater number of tests including strain path changes. Therefore, the use of such mixed models shall be required only if the simulation includes non-linear strain paths and the material exhibits a pronounced Bauschinger effect. New tools to help engineers choose between models could ease the spread of more advanced models in simulation of deep drawing processes when needed. With this in mind, an indicator predicting the influence of kinematic effects could help to select an adequate model.

In this study, a new indicator is introduced with the idea of characterising strain path non-linearity in order to assess kinematic hardening influence. The indicator is computed using the forming history taken from a purely isotropic simulation – which is easier to set up and parametrise. The ability of the indicator to predict inconsistencies within the isotropic simulation is investigated using U-channel simulations.

1 INTRODUCTION

Simulation techniques as finite element analysis are widely spread in sheet metal forming, as they can be help to enlarge process windows and to develop reliable tools within a short period of time. Furthermore it is well known, that accurate modelling of the material behaviour is crucial for reliable predictions of forming processes [1]. For this purpose, numerous formulations for describing complex material flow were developed in the past, requiring a greater number of tests including strain path changes.

Especially for forming processes where a high amount of cyclic bending is induced by forming through draw beads, isotropic hardening models are insufficient for precise springback prediction. Previous work already studied the influence of kinematic hardening

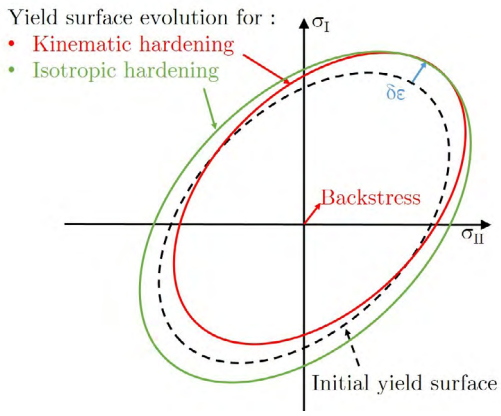

Figure 1: Kinematic and isotropic hardening

in deep drawing processes [2] and showed the importance of this material behaviour for the prediction of springback [3], being crucial for deep drawing tools design. In these cases, mixed isotropic-non-linear kinematic hardening formulations in general [4], but also special formulations of distorsional hardening as shown in [5] are able to capture the springback phenomenon. However, the authors of [6] demonstrated that identification of kinematic hardening behaviour is a difficult task due to ambiguity. Results often provide good predictions, but are not reliable in all cases and, therefore, always have to be verified. For the parametrisation of the yield surface evolution, a smart choice of experimental tests and sophisticated numerical evaluation strategies has to be made as shown in [7]. As a result of precise material modelling, it is subsequently possible to compensate springback by optimisation of tool geometries [8]. In addition to conventional strategies, the recently proposed macro-structured tools by Brosius et al. [9] are not only capable of widening process window regarding drawing depth, but are also helpful to reduce springback angles for specific materials, with a higher amount of kinematic hardening [10].

Despite the great potential for optimisation due to enhanced knowledge of kinematic hardening effects in drawing operations, in industrial applications, an estimation of the extensive efforts is often desired in advance. Additional material characterisation and numerical analysis with these models should only be performed for forming operations with high non-linear strain paths and for materials with a pronounced Bauschinger effect. For this reason evaluation tools for assisting engineers in the choice of adequate material models in simulation of deep drawing processes would be advantageous. In order to quantify non-linearity in strain paths, diverse indicators such as shown by Herault et al. [11] were proposed in the past. In this study, an alternative approach for the quantification of the kinematic hardening effect is proposed and discussed for the analysis of a macro-structured tool as used in [10].

2 CONTEXT

2.1 Hardenings models

The Bauschinger effect describe a lowering of the yield stress upon strain reversal. This change can be permanent or only transient, and the magnitude of this effect is dependent on many parameters including material and prestrain. A model aiming at the simulation of cyclic behaviour must be able to accurately capture the Bauschinger effect as shown in [12]. Strain hardening consists of a yield surface evolution following an initial deformation. The first model to capture this effect was isotropic hardening. It operates by uniformly scaling of the yield surface on increasing plastic hardening. The parameter identification of this hardening model can be realised using the result of simple tensile tests. However, this model fails to capture the Bauschinger effect, as no softening on reversal can be obtained with this family of models. Kinematic hardening was first introduced by Prager [13]. In this model, yield stress evolution is characterised by the translation of the yield surface, which is implemented using a backstress tensor. In Prager's model, backstress increments are calculated by multiplicating the strain increments by a constant c. However, the use of a pure kinematic model, does not enable a correct simulation of the Bauschinger effect within sheet metal, and a mixed model using anisotropic and kinematic hardening should be used [14].

Figure 1 represents the evolution of the yield surface following a strain increment for a isotropic hardening model and a kinematic hardening model. It is quite clear that for non-linear strain paths, the two families of models will lead to different results, in contrast to linear strain paths. Not only does kinematic hardening has a strong influence on stress values, but also on the Lankford coefficient, as the translation of the yield surface will also influence surface normals [15].

The parameter identification for non-linear, mixed models is also more complex than for isotropic models, as tension-compression tests are required. This test is challenging for sheet metal, as buckling might occur during the compression phase [16]. Besides the use of anti-buckling mechanisms supporting specimens on the surface to prevent buckling, the use of miniaturized samples, where geometry makes the tests less prone to buckling as shown in [17], is common technique.

2.2 Kinematic hardening in deep drawing processes

Non-linearity in strain path is to be expected in a deep drawing process. Indeed, the bending and unbending of the blank along the die edge implies strain reversal in the blank at least near the surface (see figure 2). However, the amount of strain path non-linearity is not easily predicted and is non-uniform in the blank for complex drawing parts. Moreover, strain path non-linerarities can be caused by other elements of the tool's geometry.

The influence of kinematic hardening in forming applications has already been studied by Oliveira et al. [18]. They investigated the influences of kinematic hardening for the U-profile and different mild and high strength steel grades (DC06 and DP600). They concluded that springback behaviour depends on strain path non-linearity. In order to study the influence of kinematic hardening, the authors compared two simulations, one imple-

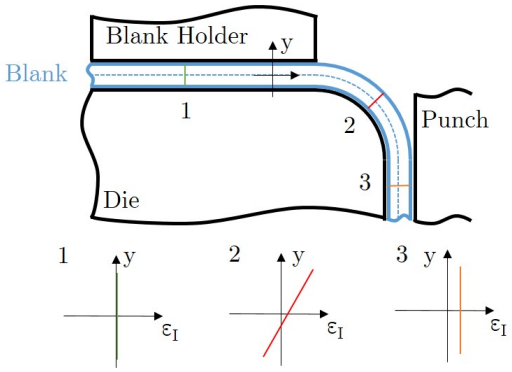

Figure 2: Strain reversal on die edge

mented a simplified isotropic model and the second used a mixed (isotropic-kinematic) hardening model. Liao et al. [3] studied the influences of path dependent behaviour on twist springback for P-channel and C-channel. They concluded that path dependent behaviour has a significant influence on simulated springback results.

2.3 Kinematic indicator

Since the influence of kinematic hardening is non-uniform and difficult to predict, a few indicators have been proposed for evaluating its influence and other strain path dependent behaviour in drawing operations.

First, Schmitt et al. [19] studied the influence of strain path change on crystal formation using the following equation:

$$\theta_{Schmitt} = \frac{\dot{\varepsilon}_1^p : \dot{\varepsilon}_2^p}{\|\dot{\varepsilon}_1^p\|\|\dot{\varepsilon}_2^p\|} \tag{1}$$

where $\dot{\varepsilon}_1^p$ and $\dot{\varepsilon}_2^p$ are two successive plastic strain increment tensors. This parameter take values between -1 and +1, with -1 corresponding to strain reversal and +1 to strain path linearity. Van Riel [20] studied the use of such indicators in FE simulations. He proposed the use of an indicator based on strains increments. However, he noted that this indicator is very sensitive to sampling frequency and converge to 1 for high enough sampling frequencies. A more stable variant was developed:

$$\theta_{VanRiel} = \frac{G : \dot{\varepsilon}^p}{\|G\|\|\dot{\varepsilon}^p\|} \tag{2}$$

where G is defined by the following differential equation:

$$\dot{G} = \dot{\varepsilon}^p - c\|\varepsilon\|G \tag{3}$$

G is named strain history and the c parameter is used to quantify the influence of previous strain states. Herault et al. [11] use this indicator to study strain reversal and cross-hardening (where yield surface is stretched perpendicularly to the strain increment) of DP600 for the reverse redrawing of cylindrical cups. A limit of this indicator is the

absence of a method to select the right value for the parameter c. Moreover, this indicator is not dependent on the material model.

Oliviera et al. [18] propose to use plastic strain direction and a plastic strain reference to develop a new indicator. However, no indication is given on how to choose the plastic strain reference. Based on this work, Clausmeyer et al. [21] introduced a cross hardening indicator and studied the influence of cross hardening for a specific channel profile.

Another proposition was made by Tekkaya at al. [22]. The authors suggest the following indicator:

$$\theta_{LWI} = \frac{\sum_{i=0}^{n}(\Delta\alpha * \delta E)}{E_{o\rightarrow\varepsilon^p_{max}}} \tag{4}$$

where α is the angle between two consecutive strain increments, and E is the plastic deformation energy. The variation of internal energy is used to weight the different changes of direction according to the amount of plastification they represent. The authors linked this indicator with kinematic influences on von Mises stress for the deep drawing of the S-Rail using DP600 steel. This indicator presented the same flaw as the discretised version of $\theta_{Schmitt}$: it is converging to zero for high enough sampling frequencies.

3 A NOVEL INDICATOR

Based on the previously introduced indicators flaws, it is possible to set some specifications for a novel indicator. The output values should be a scalar; it must have a local definition to be calculable for every element in a FE simulation. It should take values between 0 and 1 and converge as the sampling frequency increases.

The following new indicator is proposed :

$$\theta = \frac{\sum_{i=0}^{N} \measuredangle(\alpha_{est}, \dot{\varepsilon}^p) * \delta E}{\pi * w_{max}} \tag{5}$$

where:

- α_{est} is the estimation of the backstress tensor
- δw is the variation of the specific plastic work for the given timestep
- w_{max} is the maximum of the specific plastic work in the part

The angle between the backstress tensor and the plastic strain is defined between 0 and π. This value is meant to represent the non-linearity of the strain path at specific time of the simulation. The use os specific plastic work increment enables to weight the most important evolution of the strain history. The backstress estimation α_{est} is calculated using the strain path produced by an isotropic simulation using:

$$d\alpha_{est} = \dot{\varepsilon}^p * \frac{d\sigma_0}{d\varepsilon^p_{eq}} \tag{6}$$

The backstress is estimated using the hardening law and the strain path, assuming a pure kinematic model. It is therefore possible to validate the convergence condition

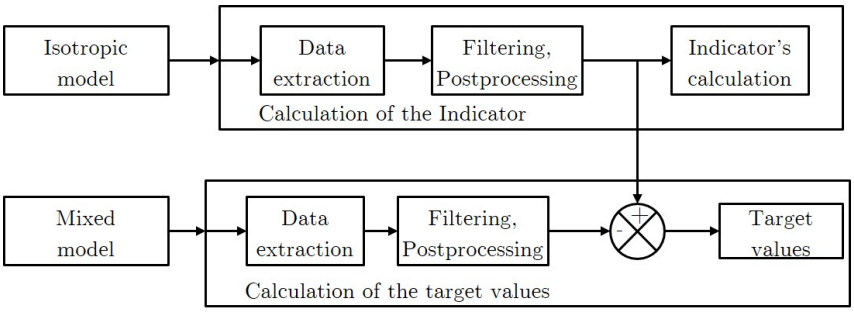

Figure 3: Calculation of indicator and target values

without having specified a fixed reference such as Oliviera et al. [18] or a value constructed from unspecified parameters such as Van Riel [20].

A shell element has different layers, corresponding to different integration points along the section. The strain history depends of the chosen integration point. Therefore, the indicator must be calculated for each integration point. With the software (LS-DYNA) used in this work, three integration point can be used: upper, middle and lower.

4 EVALUATION OF THE INDICATOR

4.1 Evaluation framework

To validate the use of this indicator, a scheme presented figure 3 was employed. First, two simulations are carried out using LS-DYNA; one with a full isotropic model, and a second with a mixed model. Then the isotropic simulation results are used to calculate the indicator. Disparities between two simulations are then used as target value: the deviation between the two simulations is subsequently used as a measure of the influence of kinematic hardening. Different target variables may be used. This work focus on specific accumulated plastic work and von Mises equivalent stress. Both are dependent on the integration point and should be compared with the corresponding value of the indicator, i.e. calculated for the same integration point.

To evaluate the performance of this indicator, a simple U-profile shape is used at first. To create more complex strain paths, macro-structured tools are used. Introduced by Brosius et al. [9] to enable lubricant free deep drawing, the U-profile tool consists of a macro-structured blank holder and die as shown in Figure 4. With this tool, the immersion depth δ (see figure 4), which is the distance between blankholder and die substracted from blank thickness is adjustable. Two configurations will be used in this paper, an immersion depth of $0mm$ and $0.2mm$. The indicator, as well a the target values, should show a significant sensitivity to these features (macro-structured, immersion) of the tool for materials with pronounced kinematic hardening. The material used is an DP600 steel. Sheet thickness was mesured at 1,17mm. Drawing Depth was 90mm. Other geometric properties are shown figure 4.

The simulation are performed using LS-DYNA 11.0.0 using MPP for parallelisation. A high number of elements were used (around 15000 in the blank), as the used proprocessing

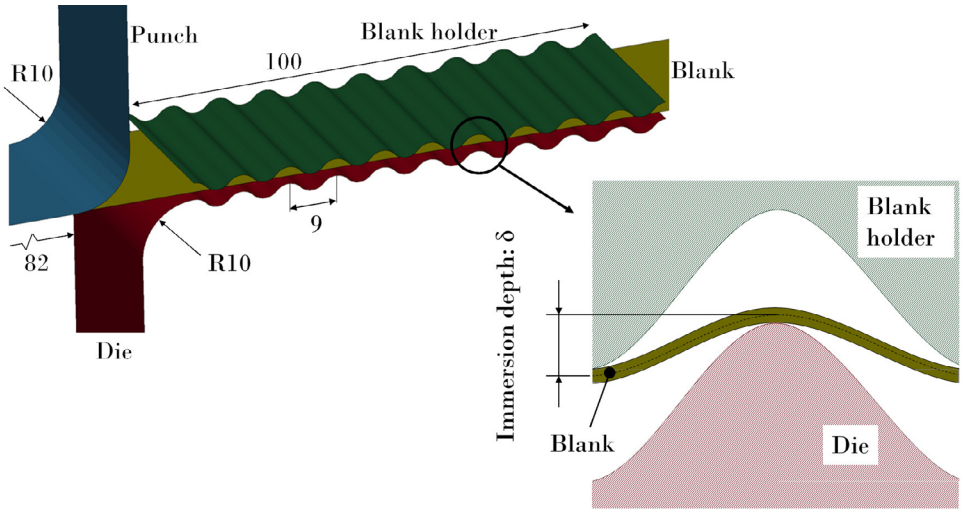

Figure 4: Tools and blank in LS-PREPOST

Table 1: DP600 Parameter for Simulation

Parameter description	Symbol	Value	Unit
Young's Modulus	E	185	MPa
Mass density	ρ	7850	kg^{-3}
Poisson coefficient	ν	0.3	$\varnothing$
Swift parameter	ε_0	$1.822 * 10^{-3}$	$\varnothing$
Swift parameter	k	1060	MPa
Swift parameter	n	0.1741	$\varnothing$
Chaboche modified parameter	a_1	379.0	MPa
Chaboche modified parameter	c_1	11.40	$\varnothing$

libraries are not compatible with active remeshing. Belytschko-Tsay formulation was used ($ELFORM = 2$) with 9 integration point. The material model used is a modified Chaboche (**MAT_133*), for both mixed and isotropic model. The Barlat 2000-2d yield criterion is used.

Computation of the indicator is performed in Python using SciPy [23], and qd.cae[1].

For the material characterisation of the DP600, tensile tests in three different rolling directions, a bulge test and a cyclic tension compression test were carried out and used for parameter identification.

4.2 Performance of the indicator

At first, numerical results of the macrostructured U-profile drawing with zero immersion depth ($\delta = 0mm$) depth will be investigated. The figure 5 represents the von Mises equivalent stress for different integration points. Figure 6 represents the differences of the von Mises equivalent stress values between the simulations implementing isotropic and

[1]https://github.com/qd-cae/qd-cae-python

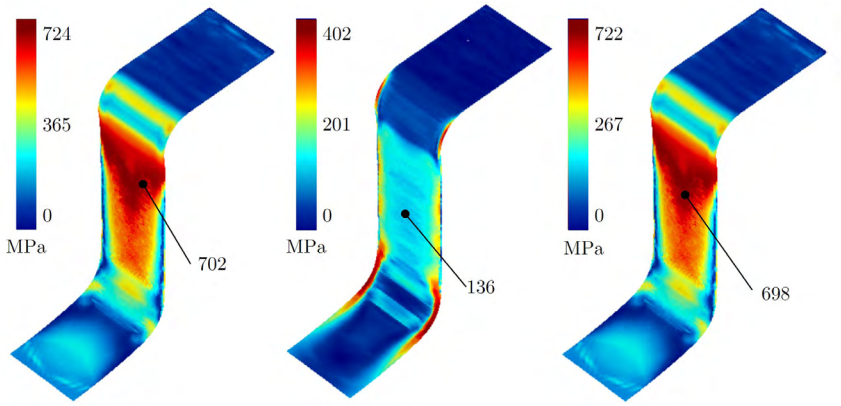

(a) Upper layer (b) Middle layer (c) Lower layer

Figure 5: Values of the von Mises stresses values ($\sigma_{\text{VM, Iso.}}$) for different layers and with a zero immersion depth ($\delta = 0mm$)

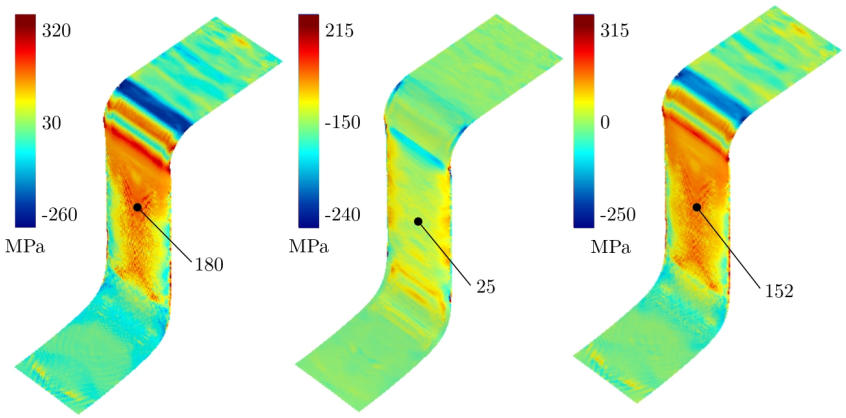

(a) Upper layer (b) Middle layer (c) Lower layer

Figure 6: Values of the difference between simulation for von Mises stresses values ($\sigma_{\text{VM, Iso.}} - \sigma_{\text{VM, Kin.}}$) for different layers and with a zero immersion depth ($\delta = 0mm$)

combined isotropic-kinematic hardening model. The figure 7 represents the specific plastic work for the two simulation, and the difference obtained, for the upper layer. Those results are consistent with theory: the influence of kinematic hardening is linked with the bending and unbending along the die radius. As expected, the plastic works after unbending is smaller for the mixed model than for the isotropic model, despite being the same after the first bending.

The figure 8 represents the values obtained for the indicator on different layer. Results imply the indicator is able to accurately predict differences between accumulated specific plastic work. However, it is less suitable for predicting discrepancies concerning the von Mises stress. This is linked to the accumulative definition of the indicator, leading to steadily increasing or constant values, which therefore cannot predict a reduction of stress values. Another error source is likely caused by strain path differences: this indicator can be useful only for process simulations where the characteristics of the strain paths are

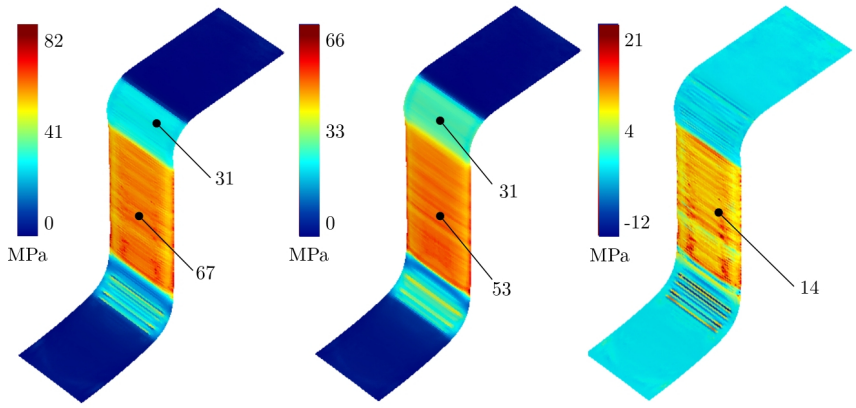

(a) Isotropic model (b) Mixed model (c) Difference

Figure 7: Values of the specific accumulated plastic work in the upper layer for the simulation implementing the isotropic model (a), the mixed model and differences between simulation ($w_{\text{pl, Iso.}} - w_{\text{pl, Kin.}}$) for the Upper layer and with a zero immersion depth ($\delta = 0mm$)

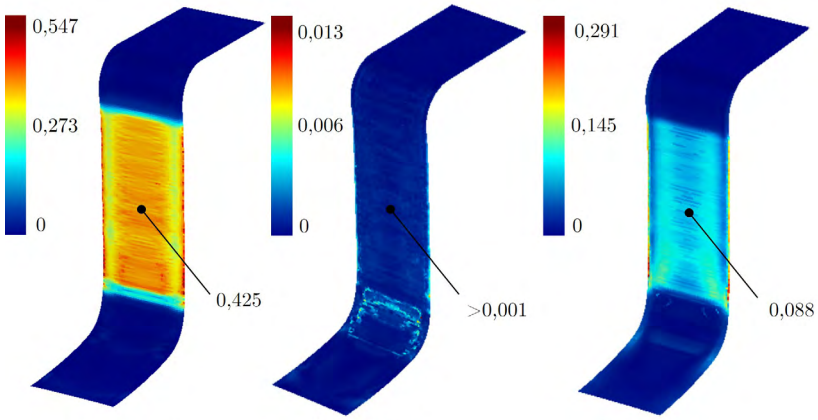

(a) Upper layer (b) Middle layer (c) Lower layer

Figure 8: Values of the indicator θ for different layers and with a zero immersion depth ($\delta = 0mm$)

relatively insensitive regarding the used material model.

When immersion depth is high enough that plastification occurs between blank holder and die, kinematic hardening will play a major role, as bending and unbending occurs in a significant number of times. Figure 9 represents the numerical results computed with a non-zero immersion depth. As expected for this immersion depth, plastification occurs within the blank, which is is visible figure 9 (a). The alternate bending in this zone result in large differences between the two simulations, especially concerning the plastic work as shown figrure 9 (b). Indeed, the upper and lower layers of blank are constantly submitted to reversed loading and deformation. The indicator is able to correctly capture this effect, as presented Figure 9 (c).

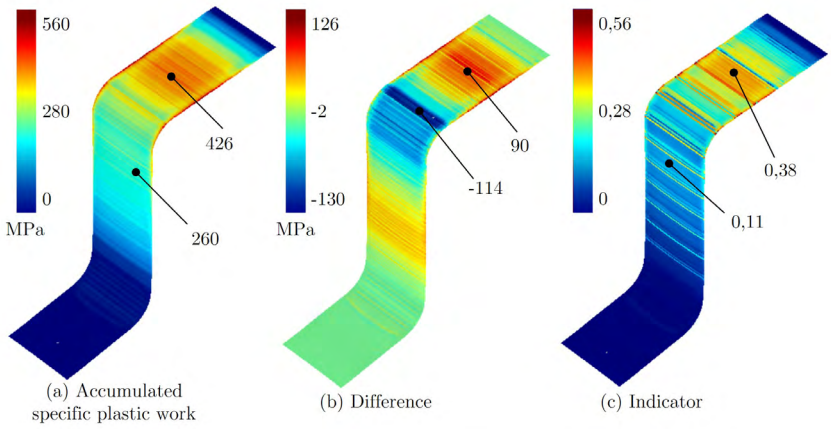

(a) Accumulated specific plastic work (b) Difference (c) Indicator

Figure 9: Values of the specific accumulated plastic work in the upper layer for the simulation implementing the isotropic model (a), the differences between both simulation ($w_{\text{pl, Iso.}} - w_{\text{pl, Kin.}}$) (b), and the indicator (θ)(c) for the upper layer and with non-zero immersion depth ($\delta = 0.2mm$)

5 CONCLUSION

In this work, the importance of the kinematic hardening influence is recalled within deep drawing simulation. Based on previous work, a new indicator to predict the influences of kinematic hardening using isotropic simulation results has been proposed. Unlike previous indicators, it is stable for increasing sampling frequencies, but does not require any references or other parameter. Using the additional information provided by the indicator, engineers are able to evaluate material's choice and tool design in early stages of process design and furthermore conclude on the necessity of extensive material characterisation for kinematic hardening for specific forming operations.

The ability of this indicator to predict kinematic hardening has been illustrated using FE-simulation. Future studies will focus on the confirmation of the performance of this new indicator for different, more complex shaped parts. A method to find the smallest sampling frequencies will be investigated. Further developments of the indicator will also be related to springback quantification and an evaluation regarding process limits.

6 ACKNOWLEDGMENT

The authors are grateful to the German Federation of Industrial Research Associations (AiF) for supporting the research project "Relevance analysis for the kinematic hardening in deep drawing processes with closed profiles" (IGF 19973BG). The computations were performed on a PC-Cluster at the Center for Information Services and High Performance Computing (ZIH) at TU Dresden.

REFERENCES

[1] Bruschi, S., Altan, T., Banabic, D., Bariani, P.F., Brosius, A., Cao, J., Ghiotti, A.,Khraisheh, M., Merklein, M., Tekkaya, A.E. (2014) *Testing and modelling of material behaviour and formability in sheet metal forming.* CIRP Ann – Manuf Techn

63/2:727-749.

[2] Haddag, B., Balan, T., and Abed-Meraim, F. (2007). *Investigation of advanced strain-path dependent material models for sheet metal forming simulations.* International Journal of Plasticity, 23(6), 951–979. https://doi.org/10.1016/J.IJPLAS.2006.10.004

[3] Liao, J., Xue, X., Lee, M.-G., Pereira, A. B., Barlat, F., Vincze, G., and Pereira, A. B. (2017). *Constitutive modeling for path-dependent behavior and its influence on twist springback.* International Journal of Plasticity, 93, 64–88. https://doi.org/10.1016/j.ijplas.2017.02.009

[4] Taherizadeh, A., Ghaei, A., Green, D. E., and Altenhof, W. J. (2009). *Finite element simulation of springback for a channel draw process with drawbead using different hardening models.* International Journal of Mechanical Sciences, 51(4), 314-325.

[5] Lee, J. Y., Lee, J. W., Lee, M. G., and Barlat, F. (2012). *An application of homogeneous anisotropic hardening to springback prediction in pre-strained U-draw/bending.* International Journal of Solids and Structures, 49(25), 3562-3572.

[6] Eggertsen, P. A., and Mattiasson, K. (2011). *On the identification of kinematic hardening material parameters for accurate springback predictions.* International journal of material forming, 4(2), 103-120.

[7] Avril S, Bonnet M, Bretelle AS, Grédiac M, Hild F, Ienny P, Latourte F, Lemosse D, Pagano S, Pagnacco E, Pierron F (2008) *Overview of Identification Methods of Mechanical Parameters Based on Full-field Measurements.* Experimental Mechanics 48(4):381.

[8] Meinders, T., Burchitz, I. A., Bonté, M. H., and Lingbeek, R. A. (2008). *Numerical product design: Springback prediction, compensation and optimization.* International Journal of Machine Tools and Manufacture, 48(5), 499-514.

[9] Brosius, A., and Mousavi, A. (2016). *Lubricant free deep drawing process by macro structured tools.* CIRP annals, 65(1), 253-256.

[10] Mousavi, A., Ridolfi, K. S., and Brosius, A. (2018). *Influence of alternating bending on springback behavior of parts in deep drawing process with macro-structured tools.* In MATEC Web of Conferences (Vol. 190, p. 14005). EDP Sciences.

[11] Herault, D., Thuillier, S., Manach, P.-Y., and Duval, J.-L. (2018). *Strain path changes in Reverse Redrawing of DP Steels.* IOP Conference Series: Materials Science and Engineering, 418(1), 012042. https://doi.org/10.1088/1757-899X/418/1/012042

[12] Choteau, M. (1999). *Caractérisation de l'effet bauschinger en sollicitations uniaxiales d'un acier inoxydable austenitique X2CrNiMo17-12-2.*. Retrieved from https://www.theses.fr/1999LIL10209

[13] Prager, W. (1949). *Recent Developments in the Mathematical Theory of Plasticity.* Journal of Applied Physics, 20(3), 235–241. https://doi.org/10.1063/1.1698348

[14] Chun, B. K., Jinn, J. T., and Lee, J. K. (2002). *Modeling the Bauschinger effect for sheet metals, part I: Theory.* International Journal of Plasticity, 18(5–6), 571–595. https://doi.org/10.1016/S0749-6419(01)00046-8

[15] Wagoner, R. H., Lim, H., and Lee, M.-G. (2013). *Advanced Issues in springback.* International Journal of Plasticity, 45, 3–20. https://doi.org/10.1016/J.IJPLAS.2012.08.006

[16] Boger, R. K., Wagoner, R. H., Barlat, F., Lee, M. G., and Chung, K. (2005). *Continuous, large strain, tension/compression testing of sheet material.* International Journal of Plasticity, 21(12), 2319–2343. https://doi.org/10.1016/j.ijplas.2004.12.002

[17] Staud, D., Merklein, M., Borsutzki, M., and Geisler, S. (2009). *Zug-Druck-Versuche an Miniaturproben zur Erfassung von Parametern für kinematische Verfestigungsmodelle.* Tagungsband Werkstoffprüfung, 2, 211-218.

[18] Oliveira, M. C., Alves, J. L., Chaparro, B. M., and Menezes, L. F. (2007). *Study on the influence of work-hardening modeling in springback prediction.* International Journal of Plasticity, 23(3), 516–543. https://doi.org/10.1016/J.IJPLAS.2006.07.003

[19] Schmitt, J. H., Aernoudt, E., and Baudelet, B. (1985). *Yield loci for polycrystalline metals without texture.* Materials Science and Engineering, 75(1–2), 13–20. https://doi.org/10.1016/0025-5416(85)90173-9

[20] Van Riel, M. (2009, August 28). *Strain path dependency in sheet metal. Experiments and models.* Retrieved from https://research.utwente.nl/en/publications/strain-path-dependency-in-sheet-metal-experiments-and-models

[21] Clausmeyer, T., Güner, A., Tekkaya, A. E., Levkovitch, V., and Svendsen, B. (2014). *Modeling and finite element simulation of loading-path-dependent hardening in sheet metals during forming.* International Journal of Plasticity, 63, 64–93. https://doi.org/10.1016/J.IJPLAS.2014.01.011

[22] A. E. Tekkaya, M. Merklein, H. Traphöner, M. Rosenschon, *Identifikation spannungsabhängiger Bauschinger-Koeffizienten*, ISBN: 978-3-86776-480-3

[23] Jones E, Oliphant E, Peterson P, et al. (2001-). *SciPy: Open Source Scientific Tools for Python*, http://www.scipy.org/